Effects of Early Afterdepolarizations on Ventricular Tachycardia in Human Heart

Jieyun Bai[1], Kuanquan Wang[1], Qince Li[1], Yinghui Li[2], Henggui Zhang[1,3]

[1]School of Computer Science and Technology, Harbin Institute Technology, Harbin, China
[2]State Key Laboratory of Space Medicine Fundamentals and Application, Beijing, China
[3]School of Physics and Astronomy, University of Manchester, Manchester, UK

Abstract

Experimental studies suggest EADs may occur at rapid heart rates as a consequence of tachyarrhythmias. The aim of this study was to investigate the interaction between EAD and rapid reentrant excitation waves and assess its effects with electrocardiogram (ECG).The simulation results indicated that, at the cellular level, reduced repolarization reserve contributed to action potential duration (APD) prolongation (ENDO: 302ms vs. 402ms, MIDDLE: 414ms vs.>1000ms, EPI: 298ms vs. 397ms) and genesis of EADs only in MIDDLE cells. In the 3D model, EADs caused drift of rapid rotors. Multiple focal excitations arising from EADs kept regeneration of reentrant excitation waves by breaking excitation wave fronts. ECGs presented periodic features with stable re-entry in control condition, but degenerated into irregular and complex patterns in EADs condition. The simulation results demonstrate that MIDDLE cells are prone to genesis of EADs at rapid heart rates, which plays an important role in degenerating ventricular tachycardia into ventricular fibrillation.

1. Introduction

Despite dramatic improvements of medical technology in the past several decades, implantable cardioverter-defibrillator, catheter ablation and antiarrhythmic drug therapy are not yet reliable for preventing sudden cardiac death and may be a disappointment following the sobering results of clinical trials[1]. Therefore, cardiovascular disease remains the most important cause of sudden death in the world [1]. The majority of such cardiac sudden deaths are caused by ventricular arrhythmias, which were often triggered by abnormal excitations at the single cell level, such as early afterdepolarizations (EADs) [2]. Thus, understanding cardiac arrhythmia mechanisms caused by EADs is most important for clinical practices.

Early afterdepolarizations (EADs) are an important cause of lethal ventricular arrhythmias in long QT syndromes. Clinical studies have shown that sudden death is initiated by an ill-timed propagated ectopic beat that leads to fibrillation [3]. Experimental studies have demonstrated that abnormal calcium (Ca^{2+}) cycling is a critical factor in the development of focal excitations[2]. Interestingly, recent evidence suggests that EADs may occur at rapid heart rates as a sequence of spontaneous sarcoplasmic reticulum (SR) Ca^{2+} release related to intracellular Ca^{2+} overload[3,4]. It suggests that EADs is associated with ectopic beat and abnormal calcium cycling, which links EADs to ventricular fibrillation. Unfortunately, the exact mechanisms by which abnormal electrical waves of excitation caused by individual-cell events degenerate into ventricular arrhythmias are not fully understood.

A successful effort will require a multiscale approach to link events (abnormal calcium) at the protein scale (ion channels), which constitute the major biologic targets for drugs and genetic interventions, to the cardiac electrophysiological properties at the cell (EADs and DADs), tissue (spiral waves), and even organism scales (spiral waves and ECG) [5]. Fortunately, the required experimental and computational tools for the challenge are rapidly being developed. Huffaker*et al* suggested EADs related to spontaneous SR Ca^{2+} release can enhance arrhythmogenesis by reinitiating reentry with 1D and 2D homogeneous canine-tissue model [6] and also found EADs can influence the stability of reentry [7].Although they reproduced the experimental observation and investigated the ionic mechanism of genesis of EADs, their study focused on the effect in homogeneous canine-tissue model. Considering the tissue heterogeneity, Mahajan *et al*[8] and de Lange *et al*[9] found that the generation of EADs has all features of a chaotic process. And such chaotic behavior can synchronize spatially to overcome source-sink mismatches and form propagating waves in a heterogeneous rabbit-tissue model. Later, Vandersickel *et al*[10] studied wave patterns resulted from single-cell EAD dynamics in a homogeneous human-tissue model. Despite great efforts on ionic basis of EADs and its effect

on reentry waves1D and 2D tissue, the mechanisms underlying EAD-linked arrhythmogenesis remains unclear in the 3D tissue.

Considering complex geometry and anisotropic properties of ventricular tissue, we investigated effects of EADs on ventricular tachycardia in human heart. Firstly, we simulated EADs, by modifying I_{CaL} and I_{Kr} based on previous experimental results. Secondly, we investigated effects of pacing rate and heterogeneity on genesis of EADs. Thirdly, a 3D human ventricular conduction model was developed by integrating Purkinje fiber network system and anatomically detailed ventricular geometry of the human heart with detailed electrophysiology in the format of mono-domain model for simulating excitation waves at organ level. Using this model, the interaction between EADs and rapid reentrant excitation waves was simulated and its effect on electrocardiogram (ECG) was assessed. These simulation results suggest rapid rate induced single-cell EADs may cause ventricular tachycardia degenerate into ventricular fibrillation which kill patients.

2. Method and material

2.1. Mathematical model

A 3D human ventricular conduction model was developed based on the ten Tusscher and Panfilov (TP06) ventricular cell model [11]. Some parameters were modified to simulated EADs (see Table 1), based on the study of Vandersickel *et al*[10]. The cell model contains several ionic currents which have the form:

$$I_i = G_i \times m_i \times n_i \times (V - V_{rev,i}) \qquad (1)$$

Where I_i is the current of the ion channel *i*, G_i is the maximal conductance of *i* channel, m_i and n_i are gates of the *i* channel, V is the cellular membrane potential and $V_{rev,i}$ is the reversal potential for *i* channel.

A ventricular conduction system is built by coupling the cells to each other in a 3D lattice with current diffusing from one cell to its neighbours through gap junctions. This can be described as a partial differential equation:

$$C_m \partial V / \partial t = D\nabla^2 V - I_{ion} \qquad (2)$$

Where V(mV) is the transmembrane potential, C_m(pF) is the membrane capacitance, I_{ion} (pA) is the sum of ionic currents(see Formula (1)) and t(ms) is time, and D is the electronic diffusion modelling gap junction coupling. More detailed parameters and equations were documented in the TP06 model [11].

Table 1. Changes of parameters for simulating EADs.

Parameters	Percentage
G_{Kr}	0.8 fold (↓)
G_{CaL}	6 fold (↑)
Tau	2 fold (↓)

Note: G_{Kr} is maximal conductance of delayed outward potassium current, G_{Kr} is maximal conductance of L-type calcium current and *Tau* is the time constant of voltage-dependent inactivation of L-type calcium channel.

2.2. Pacing protocol and definitions

In this study, the bio-marks included the shape and length of action potentials. In order to investigate the effect of rapid pacing on genesis of EADs, pacing cycle length was changed from 2000ms to 500ms. And the effect was recorded in EPI cells. The susceptibility to genesis of EADs in three cell types was compared and analysed.

To induce spiral waves, the standard S1-S2 protocol was used. First of all, we applied S1 stimulus on the end of the Purkinje fiber network. Then a S2 stimulus on the endo-cardiac region was applied when the region was recovered. Finally, a spiral wave was induced.

To assess the effects of single cell EADs on whole organ spiral waves, the ECG was obtained by calculating voltage gradient from a point 2cm away from EPI layer. The principal peak of ECG was calculated by temporal Fourier transforms.

2.3. Numerical methods

The PDE models were solved by an explicit forward Euler approximation of the Laplacian operator. In the three-dimensional simulations, the time step (Δt) for ordinary differential equation solutions was 0.02 ms and the space steps (Δx and Δy) were fixed at 0.35 mm. These choices provided stability and accuracy with the chosen numerical integration method and did not disturb the conditions of medium continuity. Simulations were carried out on a system with 64 G memory and Intel core i703930K 64-bit CPU. Efficient parallelization was implemented using GPU acceleration.

3. Results

3.1. EADs induced by rapid pacing rate

In order to find the major biologic targets for drugs and genetic interventions, we investigated the susceptibility to genesis of EADs in three cell types with normal pacing rate (CL=1000 ms). Compared with the normal condition, reduced repolarization reserve induced by decreasing I_{Kr} contributed to action potential duration (APD) prolongation (ENDO: 302ms vs. 402ms, MIDDLE: 414ms vs.>1000ms, EPI: 298ms vs. 397ms) and genesis of EADs only in MIDDLE cells under the EADs

condition (not shown). Therefore, as for EADs, the MIDDLE cells may be the major biologic target.

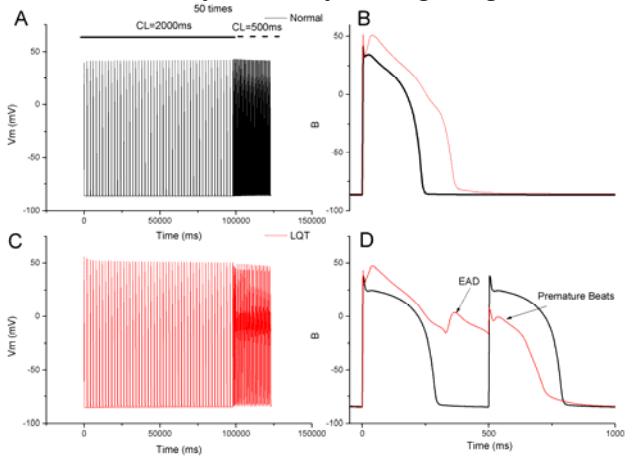

Fig1. Action potentials with pacing rate acceleration. Action potential consequence is obtained under normal (A) and EADs (C) conditions. Shape and duration of action potential are compared at CL=2000 ms (B) and CL=500 ms (D).

In order to examine the effects of pacing rate acceleration, the action potentials of EPI cells were compared under the normal and EADs conditions as shown in Fig1. With increasing pacing rate, EADs and premature beats were induced in EPI-cardiac cells. The changes of action potential profiles were investigated by changing cycle length from 2000ms to 500ms under both normal (A) and EADs conditions (C). At CL=2000ms, the action potential was significantly prolonged without inducing EADs (Fig.1B) by altering ionic channel dynamics as shown in Table 1, which is consistent with the previous experiments. However, at rapid pacing rate (CL=500 ms), EADs were induced (Fig.1.D).

3.2. Ventricular tachycardia degenerating into ventricular fibrillation due to EADs

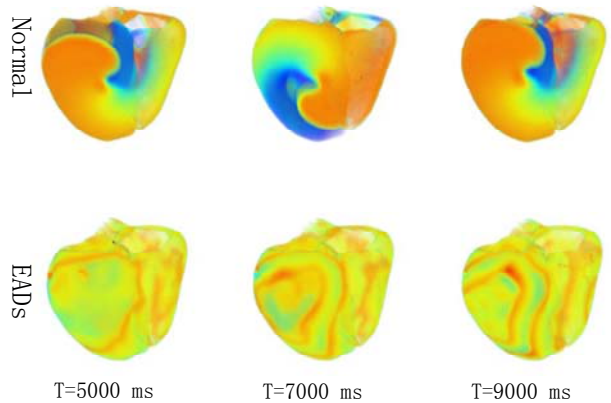

Fig2. Illustration of stable spiral wave under Normal condition and typical break formation under the EADs condition.

Spiral waves under normal and EADs conditions were induced by S1-S2 protocol (see pacing protocol and definitions) as shown in Figure 2. The snapshots demonstrated evolution of re-entrant waves arising from a premature stimulus (the S2 stimulus). For the normal condition, the spiral wave was stable and sustained throughout the simulation period (10s). However, under the EADs condition, the scroll wave was unstable and broken into multi-wavelets (from 5000ms, 7000ms to 9000ms).

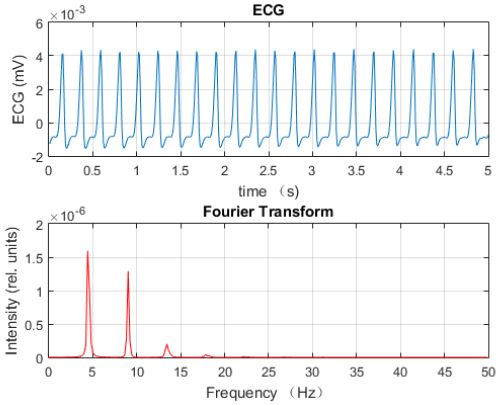

Fig.3. ECG and Fourier Transform under normal condition.

In order to illustrate the relationship between unstable spiral wave and the pro-arrhythmic effects of the EADs, the corresponding pseudo-ECG of spiral waves under normal and EADs conditions were calculated. The results are shown in Fig.3 and Fig.4. For the normal condition, the ECG was stable and orderly (Fig.3 upper layer), while under EADs condition, the ECG was not regular (Fig.4 upper layer). In addition, power spectrum analysis of the recorded electrical activity from the tissue revealed a dominant frequency of 4.4Hz and 5.62Hz for the normal and EADs conditions, respectively (bottom layers in Fig.3 and Fig.4). Compared with that under normal condition, the dominant frequency of pseudo-ECG under the EADs condition was higher.

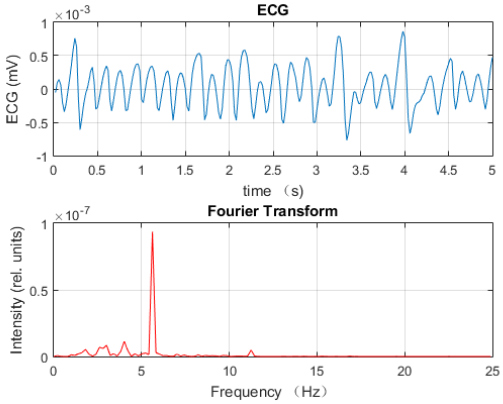

Fig.4. ECG and Fourier Transform under EADs condition.

The pseudo-ECG and power spectrum analysis connected the simulations with clinical observation. These results are consistent with clinical observation of LQT patients.

In order to further illustrate the ventricular arrhythmias due to the individual-cell events, we compared action potentials in ENDO, MIDDLE and EPI cells in the human heart. It is found that all the action potentials in all 3 types of cells were prolonged, whereas EADs was only observed in MIDDLE cells (not shown). These results are consistent with the simulation in single cell level, implicating single cell EADs influenced the stability of spiral waves and induced ventricular tachycardia to degenerate into ventricular fibrillation.

4. Discussions and conclusion

The decrease of I_{Kr} can reduced repolarization reserve for APD prolongation and the increase of I_{CaL} contributed to Ca^{2+} overload and spontaneous sarcoplasmic reticulum (SR) Ca^{2+} release for EADs.The simulation results showed that compared with other cell types, the MIDDLE cells were prone to genesis of EADs. In the 3D model, EADs caused drift of rapid rotors. Multiple focal excitations arising from EADs induced persistent regeneration of reentrant excitation waves by breaking excitation wave fronts. The principal peak of ventricular tachycardia (Normal) was greater than that of ventricular fibrillation (EADs). In addition, ECGs presented periodic features with stable reentry in control condition, but degenerated into irregular and complex features in EADs condition. These observations were characteristic of the differences between ventricular tachycardia and ventricular fibrillation, which are in good agreement with clinical reports. The simulation results suggest that MIDDLE cells are prone to genesis of EADs at rapid heart rates, which plays an important role in degenerating ventricular tachycardia into ventricular fibrillation.

Acknowledgements

This work is supported by the National Natural Science Foundation of China (NSFC) under Grant No. 61571165and No. 61572152.

References

[1]. Turakhia MP. Sudden cardiac death and implantable cardioverter-defibrillators. American family physician 2010;82:1357-66.

[2]. Gaztañaga L, Marchlinski FE, Betensky BP. Mechanisms of cardiac arrhythmias. Revista Española de Cardiología (English Edition) 2012;65:174-85.

[3]. Shiferaw Y, Aistrup GL, Wasserstrom JA. Intracellular Ca2+ waves, afterdepolarizations, and triggered arrhythmias. Cardiovascular research 2012;95:265-8.

[4]. Song Z, Ko CY, Nivala M, Weiss JN, Qu Z. Calcium-Voltage Coupling in the Genesis of Early and Delayed Afterdepolarizations in Cardiac Myocytes. Biophysical journal 2015;108:1908-21.

[5]. Weiss JN, Garfinkel A, Karagueuzian HS, Chen P-S, Qu Z. Early afterdepolarizations and cardiac arrhythmias. Heart Rhythm 2010;7:1891-9.

[6]. Huffaker R, Lamp ST, Weiss JN, Kogan B. Intracellular calcium cycling, early afterdepolarizations, and reentry in simulated long QT syndrome. Heart Rhythm 2004;1:441-8.

[7]. Huffaker RB, Weiss JN, Kogan B. Effects of early afterdepolarizations on reentry in cardiac tissue: a simulation study. American Journal of Physiology-Heart and Circulatory Physiology 2007;292:H3089-H102.

[8]. Mahajan A, Shiferaw Y, Sato D, et al. A rabbit ventricular action potential model replicating cardiac dynamics at rapid heart rates. Biophysical journal 2008;94:392-410.

[9]. de Lange E, Xie Y, Qu Z. Synchronization of early afterdepolarizations and arrhythmogenesis in heterogeneous cardiac tissue models. Biophysical journal 2012;103:365-73.

[10]. Vandersickel N, Kazbanov IV, Nuitermans A, Weise LD, Pandit R, Panfilov AV. A study of early afterdepolarizations in a model for human ventricular tissue. PloS one 2014;9:e84595.

[11]. ten Tusscher KH, Panfilov AV. Alternans and spiral breakup in a human ventricular tissue model. American Journal of Physiology-Heart and Circulatory Physiology 2006;291:H1088-H100.

Address for correspondence.

Kuanquan Wang
Mailbox 332, Harbin Institute of Technology Harbin, China
wangkq@hit.edu.cn